

Vortex assisted mechanism of photon counting in superconducting nanowire single photon detector revealed by external magnetic field

D.Yu. Vodolazov^{1,2}

¹ *Institute for Physics of Microstructure, Russian Academy of Sciences, 603950, Nizhny Novgorod, GSP-105, Russia*

² *Lobachevsky State University of Nizhny Novgorod,
23 Gagarin Avenue, 603950 Nizhny Novgorod, Russia*

Yu.P. Korneeva³, A.V. Semenov^{3,4}, A.A. Korneev^{3,4,5}, G.N. Goltsman^{3,5}

³ *Moscow State Pedagogical University, 119991, 1 M. Pirogovskaya st., Moscow, Russia*

⁴ *Moscow Institute of Physics and Technology, 141700,
Moscow region, Dolgoprudny, 9 Institutsky lane, Russia*

⁵ *National Research University – Higher School of Economics, 101000, 20 Myasnitskaya st., Moscow, Russia*

(Dated: July 18, 2018)

We use external magnetic field to probe the detection mechanism of superconducting nanowire single photon detector. We argue that the hot belt model (which assumes partial suppression of the superconducting order parameter Δ across the whole width of the superconducting nanowire after absorption of the single photon) does not explain observed weak field dependence of the photon count rate (PCR) for photons with $\lambda=450$ nm and noticeable *decrease* of PCR (with increasing the magnetic field) in some range of the currents for photons with wavelengths $\lambda=450-1200$ nm. Found experimental results for all studied wavelengths $\lambda=450-1550$ nm could be explained by the vortex hot spot model (which assumes partial suppression of Δ in the area with size smaller than the width of the nanowire) if one takes into account nucleation and entrance of the vortices to the photon induced hot spot and their pinning by the hot spot with relatively large size and strongly suppressed Δ .

PACS numbers:

I. INTRODUCTION

The main idea of superconducting nanowire single photon detector (SNSPD) is based on destruction of the superconductivity by the absorbed high-energy photon (which produces hot quasiparticles) in relatively large area of the superconducting nanowire [1]. The appearance of such a region decreases the superconducting properties of the nanowire and leads to the resistive state (if transport current I exceeds some critical value) which is visible via appearance of the voltage. First realization of such a detector was done in 2001 [2] and since that time there were many theoretical [3–9] and experimental works (for review see [10]) which were aimed to understand the physical details of their working mechanism and to improve their characteristics.

Despite clear main idea why SNSPD works there are still debates about details of the appearance of the resistive state in SNSPD. These debates are connected with absence of rigorous study (which needs solution of kinetic equations coupled with equation for superconducting order parameter) of initial stage of the response of the superconducting nanowire on the absorbed photon. In the set of theoretical works [1, 3, 7, 8] authors used approach, which is similar to Rothwarf-Taylor model [11] and those quantitative validity is questionable in case when there is spatial gradient of superconducting order parameter Δ . Nevertheless in the literature one may find two ideas about what happens after photon absorption: the photon creates hot spot or hot belt. According to the hot spot

model absorbed photon creates region with locally suppressed superconductivity (partially or completely) with the size smaller than the width of the nanowire [3–5, 7–9]. As a result the superconducting current has to crowd near the hot spot and in Refs. [5, 8, 9] it is argued that the superconducting state becomes unstable at the current $I > I_{det}$ (which is smaller than the critical current of the nanowire without hot spot) due to nucleation and motion of the vortices.

Authors of the hot belt model [6] assume that the absorbed photon creates the spatially uniform distribution of hot quasiparticles across whole width of the nanowire and it results in the appearance of some kind of weak link. The critical current I_c^{belt} of the nanowire with hot belt (weak link) is smaller than the critical current of the nanowire I_c and when $I_c^{belt} < I < I_c$ the resistive state is realized after absorption of the photon. Vortices are involved in the hot belt model in order to explain smooth dependence of the detection efficiency (DE) of SNSPD on the applied current (seen in all experiments on SNSPD) – the finite DE at $I < I_c^{belt}$ in this model is connected with thermoactivated vortex entrance via edges of the nanowire and their motion heats the nanowire and provides large voltage response. Note that in the hot spot model considered in Ref. [9] the smooth dependence $DE(I)$ follows not only from the thermoactivated vortex entrance to the hot spot but also from dependence of I_{det} on the transverse coordinate x of hot spot in the nanowire.

In further we use term intrinsic detection efficiency (IDE), which describes probability to have the resistive

TABLE I: Material and physical properties (at $T = 1.7K$) of studied NbN based SNSPD.

Sample	w(nm)	d(nm)	$T_c(K)$	$I_c(0)(\mu A)$	$R_{sq}(Ohm)$	$\xi(nm)$	$I_{dep}^{th}(\mu A)$	β_{exp}	β_{th}
NbN1	102	4	10.1	27.1	512	4.9	44	108	208
NbN2	90	6	9.9	21.2	456	4.7	45	85	227
NbN3	110	5	9.2	25.1	420	4.7	57	83	232

response in the superconducting nanowire after photon absorption (IDE= 1 means that each absorbed photon produces resistive response). Detection efficiency in real detectors is always smaller than IDE because absorption in the detector is less than unity. With this definition IDE is the intrinsic characteristic of the superconducting nanowire and not the whole detection system. Experimentally dependence IDE(I) could be found if the photon count rate (PCR) saturates at large currents and IDE(I)=PCR(I)/PCR_{sat}.

To distinguish experimentally which of these two models is more relevant to the detection mechanism of SNSPD one may use external magnetic field. Hot belt model predicts parallel shift of dependence PCR(I) (or IDE(I)) in direction of small currents with increasing magnetic field. This result directly comes from decay of I_c^{belt} in the magnetic field – well know result following from the theory of Josephson junctions [12] and narrow superconducting films [13]. The hot spot model of Ref. [9] predicts more complicated behavior, with noticeable shift of IDE(I) at low currents (where finite $IDE \ll 1$ is assumed to be finite due to thermoactivated vortex entrance to the hot spot - like in the hot belt model) and much weaker field dependence at the currents where $IDE \gtrsim 0.1$ and vortices appears in the nanowire at the current $I > I_{det}(x)$ without any fluctuations. Moreover this model predicts *decrease* of PCR at the currents, where PCR saturates.

Recent experiment on MoSi based SNSPD [14] discards the hot belt model for this detector. It was found that for high energy photon ($\lambda = 450$ nm) detection efficiency practically did not vary in the wide range of the magnetic fields both at the currents where $IDE \ll 1$ and $IDE \sim 1$. This result also discards the possibility of photon detection via thermoactivated vortex entry in the hot spot model of Ref. [9]. For photons with larger wavelength ($\lambda=600-1000$ nm) in Ref. [14] dependence $DE(I)$ shifted in direction of smaller currents with increase of

the magnetic field. The found result – the larger λ the larger shift is also in contrast with prediction of the hot belt model where one could expect larger dependence on magnetic field for photons with larger energy (in this case Δ should be suppressed stronger in the hot belt region and one needs smaller magnetic field to suppress I_c^{belt}). In Ref. [9] no study was made for field-dependent IDE for photons with different energies.

In the present work we study effect of the magnetic field on dependence PCR(I) of SNSPD based on NbN. Among different studied detectors there was one which had saturation of PCR(I) in large range of the wavelengths $\lambda = 450-1000$ nm. Note, that for MoSi based SNSPD in Ref. [14] the saturation of PCR(I) was observed only for photons with $\lambda = 450$ nm but it was not fully complete (PCR still slightly increased with current increase). Qualitatively for all studied NbN detectors we find the same results as for the MoSi based SNSPD. Besides due to high quality of one of the studied detectors (mentioned above) we find effect which was not observed for MoSi SNSPD and which was theoretically predicted in Ref. [9] – external magnetic field decreases PCR (when it is close to PCR_{sat} at zero magnetic field) and shifts the current where PCR saturates to larger values. To explain different field dependence of PCR(I) (IDE(I)) observed for different wavelengths both for MoSi and NbN detectors we modified the hot spot model of Ref. [9] and assumed that the resistive state starts only if the vortex, which enters the hot spot via edge of the nanowire, can freely pass the hot spot region (i.e. it should be unpinned). Using this assumption and the model of Ref. [9] we were able to explain observed field dependence of PCR(I) at all studied wavelengths for both materials.

II. EXPERIMENT

In our experiments we used a cryoinsert with superconducting solenoid for the storage dewar in which operation temperature 1.7 K was achieved by helium vapor evacuation. The magnetic fields from 0 to 425 mT were applied perpendicular to the SNSPD plane. The SNSPD was fixed to a sample holder in a dipstick and was wire-bounded to a transmission line with a coplanar-

coaxial connector. The SNSPD-chip with the transmission line was connected to DC+RF-output port of a bias-T. DC port was connected with precision voltage source. Absorption of a photon produces a voltage pulse which is amplified by two room-temperature amplifiers Mini-Circuits ZFL-1000LN+ (1 GHz band, 46 dB total amplification) and it is fed to a digital oscilloscope and a

pulse counter. We recorded the count rate during an 1 s interval at each current. As a light source we used a grating spectrometer with a black body for wavelength from 400 to 1550 nm. The light is delivered to the SNSPD by an optical fiber SMF-28e with 9 μm mode field diameter. The meanders were precisely aligned against the fiber core and illuminated from the top side.

We studied three NbN detectors with different material and physical parameters (see the table 1). Only one of the detectors (NbN1) shows well determined saturation of the photon count rate at large currents in wide range of wavelengths $\lambda = 450 - 1000$ nm (see Fig. 1) and we mainly present results for this detector. In Fig. 1 we use linear scale to demonstrate the clear saturation of PCR and maximal IDE $\simeq 1$. Only for wavelengths $\lambda = 1200$ and 1550 nm intrinsic detection efficiency $\text{IDE} = \text{PCR}(I)/\text{PCR}_{\text{sat}}$ does not reach unity (for these wavelengths we find PCR_{sat} by extrapolation of the experimental data at larger currents using similarity between shapes of $\text{PCR}(I)$ for different wavelengths - see Fig. 1).

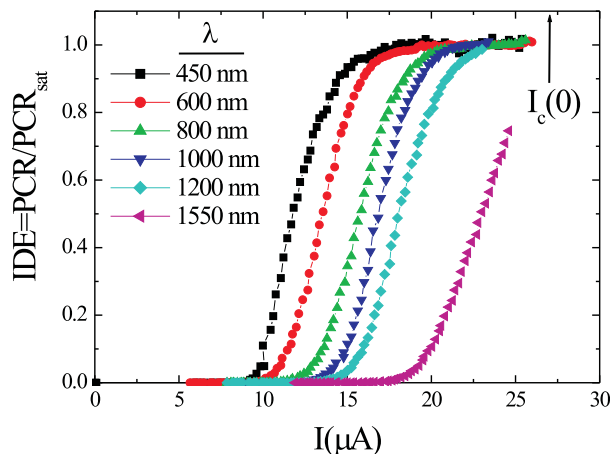


FIG. 1: Current dependence of the normalized photon count rate ($\text{PCR}/\text{PCR}_{\text{sat}}(H=0)=\text{IDE}$) for different wavelengths found for good quality detector NbN1. For $\lambda=1200$ and 1550 nm we find $\text{PCR}_{\text{sat}}(H=0)$ from extrapolation of the experimental results to larger currents and assuming small variation of the shape of dependence $\text{IDE}(I)$ with change of λ .

In Fig. 2 we show effect of the external magnetic field H on the photon count rate for photons with different energy (wavelength). Also as for Fig. 1 we subtract dark counts those rate rapidly grows when current approaches the critical current of the meander $I_c(H)$ (its dependence on H is shown in the inset in Fig. 2(d)). Effect of magnetic field is very similar to the one found before in Ref. [14] for MoSi detector – with increase of H dependence $\text{PCR}(I)$ shifts to the direction of *small* cur-

rents (at fixed current it means increase of PCR), and this shift is smaller the higher the energy of the photon. The new effect which was not observed before is the *decrease* of PCR (when $\text{IDE} \gtrsim 0.5$) at currents larger than some 'crossover' current I_{cross} - see Fig. 2. At large magnetic fields the effect is not visible because $I_c(H)$ rapidly decreases and dark counts interfere the photon counts before IDE reaches $\simeq 0.5$.

We observed the same crossover behavior also for other NbN detectors for photons with $\lambda=500-800$ nm when PCR saturated at $H = 0$. For MoSi detector the crossover was not found and dependence $\text{IDE}(I)$ just shifted to the direction of small currents (for this specific detector PCR did not saturate even for photons with $\lambda = 450\text{nm}$).

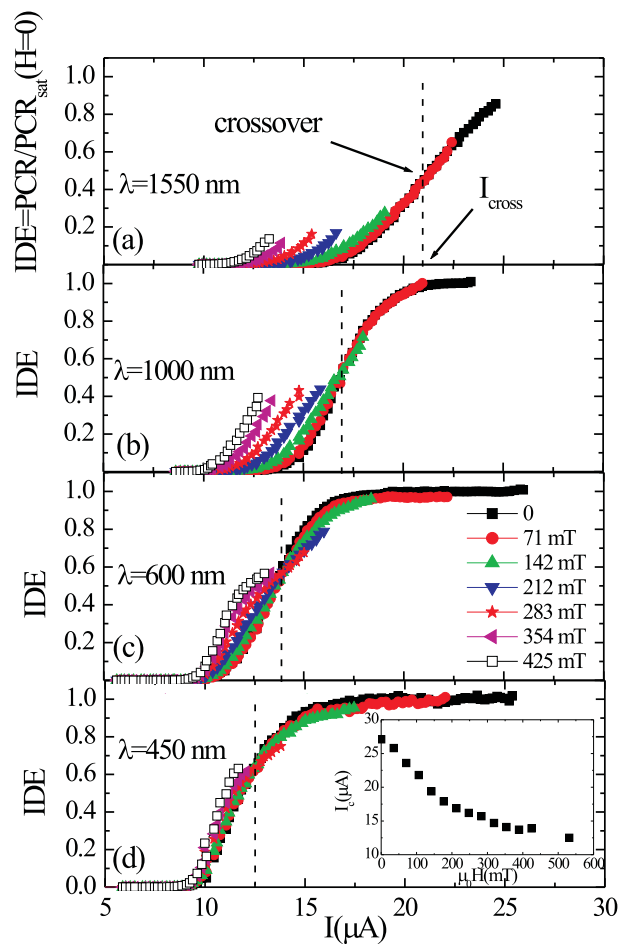


FIG. 2: $\text{IDE}(I)$ of NbN1 detector at different magnetic fields. In the inset in figure (d) we present field dependence of the critical current of the meander.

Dependence of dark count rate (DCR) on the magnetic field (see Fig. 3) is in strict contrast with the results shown in Fig. 2. DCR follows the change in the critical current of the meander and curve $\text{DCR}(I)$ shifts

to smaller currents with increasing H . Notice, that the shift is well visible even for $\mu_0 H \leq 71$ mT when photon count rate practically does not change for all studied wavelengths. On the contrary, at large magnetic fields DCR slightly depends on H (because of small change in the critical current – see inset in Fig. 2(d)), while photon count rate shows noticeable field dependence (at least for photons with $\lambda = 1000 - 1500$ nm). The present results are very similar to the results found for other NbN and MoSi detectors (see Fig. 4 below and Fig. 4 in Ref. [14]). They demonstrate that the dark counts are most probably originated from the thermo-activated vortex entrance near the 'weakest' place of the meander which determines its critical current. We may conclude it from very fast decay of DCR with the current which is consequence of large increase of the energy barrier for vortex entry δF as current decreases [15–18]. For all studied detectors the current dependence of dark count rate could be fitted by linear function $\ln(DCR) = -\beta_{exp}(1 - I/I_c(H))$ where the coefficient β_{exp} found at $H = 0$ is shown in table 1.

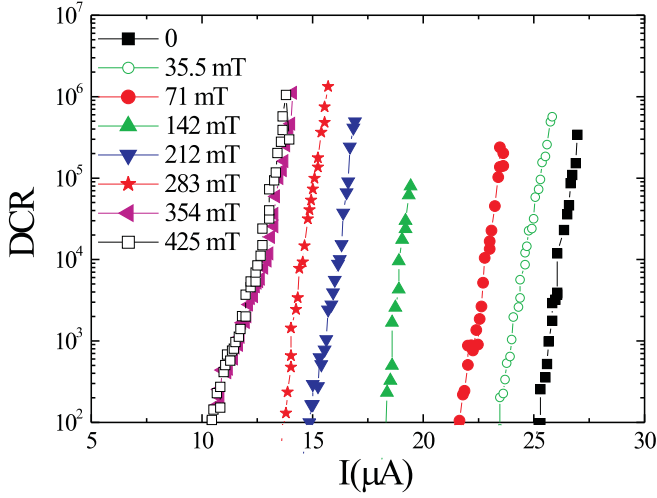


FIG. 3: Dark count rate in NbN1 detector at different magnetic fields.

Before comparison of β_{exp} with predictions of theoretical models we have to stress that the 'weakest' place could be located not only at the edges but also in the middle of straight pieces of the meander. In Fig. 4 we show dark count rate and critical current of NbN2 detector measured at different magnetic fields. One can see that at low magnetic fields ($\mu_0 H \leq 36$ mT) the critical current practically does not depend on H and DCR does so. Plateau in dependence $I_c(H)$ as $H \rightarrow 0$ may appear if there is relatively large intrinsic defect in the middle of the nanowire and resistive state starts via nucleation of the vortex-antivortex pair in that place (see discussion in section IIIB near Fig. 9). In this situation the smallest energy barrier corresponds to the nucleation of the pair vortex-antivortex near the intrinsic defect and not to the single vortex entry via edge of the nanowire.

Therefore to make quantitative comparison one needs

to know exact parameters of the 'weakest' place and where it is located in the meander. Because we do not have such an information we make rough estimation using the result following from the London model for the single vortex entry to the straight nanowire *without edge or bulk defects* $\beta_{th} = \Phi_0^2 d / 16\pi^2 \lambda_L^2 k_B T$ (see Eq. (2) in Ref. [18], where λ_L is the London penetration depth). Calculated β_{th} are shown in the table 1. One can see the large quantitative difference between β_{exp} and β_{th} which we connect with effect of unknown parameters of the 'weakest' place on value of the energy barrier.

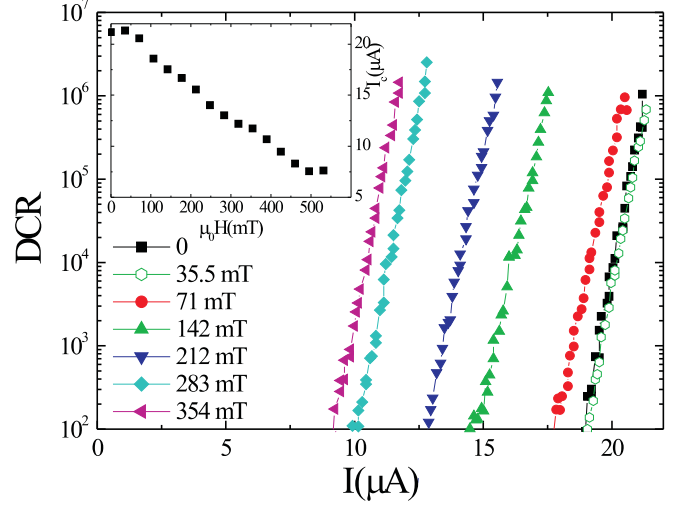


FIG. 4: Dark count rate and critical current (in the inset) of NbN2 detector at different magnetic fields.

III. THEORY

To calculate dependence $IDC(I, H)$ we use the model of Ref. [9]. The hot spot (HS) is modelled as a region in the form of a circle with radius R and inside this area the quasiparticle distribution function $f(\epsilon)$ deviates from the equilibrium (the quasiparticles are 'heated') [9]. Because of 'heated' quasiparticles the superconducting order parameter $\Delta = |\Delta|e^{i\varphi}$ is suppressed inside the hot spot and the critical current of the nanowire changes. Our aim is to find its value (we call it detection current I_{det} to distinguish it from the critical current of nanowire without hot spot) by solving the Ginzburg-Landau equation for Δ

$$\xi_{GL}^2 \left(\nabla - \frac{2ieA}{\hbar c} \right)^2 \Delta + \left(1 - \frac{T}{T_c} + \Phi_1 - \frac{|\Delta|^2}{\Delta_{GL}^2} \right) \Delta = 0. \quad (1)$$

The term [19–21]

$$\Phi_1 = \int_{|\Delta|}^{\infty} \frac{2(f^0 - f)}{\sqrt{\epsilon^2 - |\Delta|^2}} d\epsilon, \quad (2)$$

describes the effect of nonequilibrium distribution function $f(\epsilon) \neq f^0(\epsilon) = 1/(\exp(\epsilon/k_B T) + 1)$ on Δ . In Eq. (1) $\xi_{GL}^2 = \pi\hbar D/8k_B T_c$ and $\Delta_{GL}^2 = 8\pi^2(k_B T_c)^2/7\zeta(3) \simeq 9.36(k_B T_c)^2$ are zero temperature Ginzburg-Landau coherence length and superconducting order parameter correspondingly. For numerical calculations it is convenient to write Eq. (1) in dimensionless units (length is scaled in units of $\xi(T) = \xi_{GL}/(1 - T/T_c)^{1/2}$, Δ in units of $\Delta_{eq} = \Delta_{GL}(1 - T/T_c)^{1/2}$ and vector potential A in units of ξH_{c2} , where H_{c2} is the second critical magnetic field)

$$(\nabla - i\tilde{A})^2 \tilde{\Delta} + (\alpha - |\tilde{\Delta}|^2) \tilde{\Delta} = 0, \quad (3)$$

with $\alpha = (1 - T/T_c + \Phi_1)/(1 - T/T_c)$.

In our model we have two control parameters: radius of the hot spot and value of Δ inside HS (Δ_{in}), which is controlled by the parameter α in Eq. (3) (or Φ_1 in Eq. (1)). In contrast with other hot spot models (see for example Refs. [1, 3, 6–8]) our approach automatically resolves question about stability of the superconducting state of the nanowire without usage of extra assumptions (like additional condition for vortex entry needed in the London model) and it takes into account the current continuity equation $\text{div} j = 0$ (which comes from the imaginary part of Eq. (1) or Eq. (3)). Drawback of our approach is the unknown quantitative relation between the energy of the absorbed photon and the size of the hot spot and how strong Δ is suppressed inside it (strictly speaking it has to be found from the solution of the kinetic equation for $f(\epsilon)$ coupled with the equation for Δ). Despite it our theoretical results explain the experimental field dependence of the photon count rate (see results below) and it gives us the hope that the used model captures the essential physics of the detection mechanism of single photons in SNSPD.

A. Straight nanowire

In simulations we place the hot spot in different places across the straight nanowire and find dependence $I_{det}(x)$ via numerical solution of Eq. (3) (details of the numerical scheme are present in Ref. [9]). When the photon is absorbed at the edge of the nanowire we model the hot spot by a semicircle with radius in $\sqrt{2}$ times larger than radius of the hot spot inside the nanowire [5, 9]. The resistive state is realized via nucleation of the vortices (they enter via edge of the nanowire when HS is located close to the edge and vortex-antivortex pair is nucleated inside HS when it is located near a center of the nanowire) and their motion across the superconductor [9]. In Ref. [9] it was found that relatively large hot spot can pin the vortex when it enters the nanowire and one needs to enlarge current to make it unpinning. Unlike usual pinning center the hot spot relaxes in time and if it contains the vortex then at some moment in time the vortex could be unpinning and moves across the nanowire and heats it. Based on this idea the detection current in Ref. [9] was

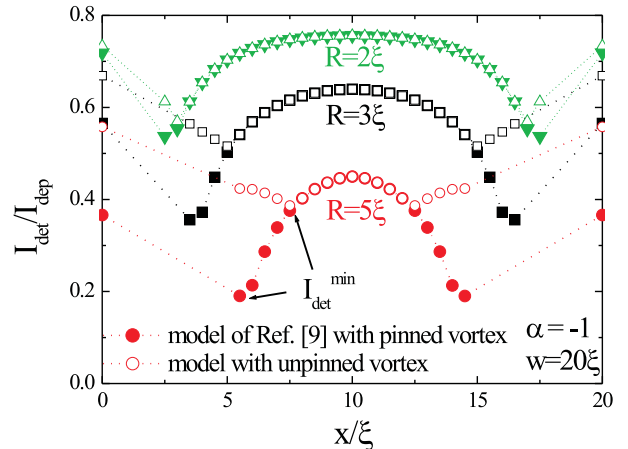


FIG. 5: Dependence of the detection current I_{det} (at which the resistive response appears in the SNSPD after photon absorption) on the coordinate of the hot spot, defined in two models: model with pinned vortex [9] (solid symbols) and model with unpinned vortex (empty symbols).

defined as a current at which the vortex enters the hot spot when it is located close to the edge of the nanowire.

In the present work we define I_{det} as the current at which the permanent motion of the vortices starts in the nanowire (i.e. vortex has to be unpinning from the hot spot). To see the difference of present definition of I_{det} with one proposed in Ref. [9], in Fig. 5 we show dependence of both I_{det} on the coordinate of the hot spot. One can see that the difference exists when the hot spot is located near the edges of the nanowire and with increase of radius of HS the difference increases. It occurs due to enhanced pinning ability of the hot spot, which in general depends also on Δ_{in} (it is controlled by the parameter α in our model). For example when $\alpha = 0$ the hot spot with $R = 2\xi$ already cannot pin vortices (at least at $H = 0$ and width of the nanowire $w = 20\xi$) and the current, at which vortex enters the hot spot coincides with the current when it becomes unpinning. For $R = 5\xi$ the hot spot cannot pin vortex nowhere in the nanowire when $\alpha \geq 0.36$ (it corresponds to $\Delta_{in} \geq 0.6\Delta_{eq}$ inside HS).

In Fig. 6 we show how I_{det} changes in the magnetic field. In the model with unpinned vortex the minimal detection current I_{det}^{min} changes slightly in weak magnetic fields ($H < H_s \simeq \Phi_0/2\pi\xi w$, with $H_s \simeq 0.05H_{c2}$ for the nanowire with $w = 20\xi$) when the radius of the hot spot is large and vortex pinning is strong. Physical reason for the found effect is following - external magnetic field favors the vortex entry to HS because of increase of the current density at one edge of the nanowire [9] but it weakly changes the current density near nanowire's cen-

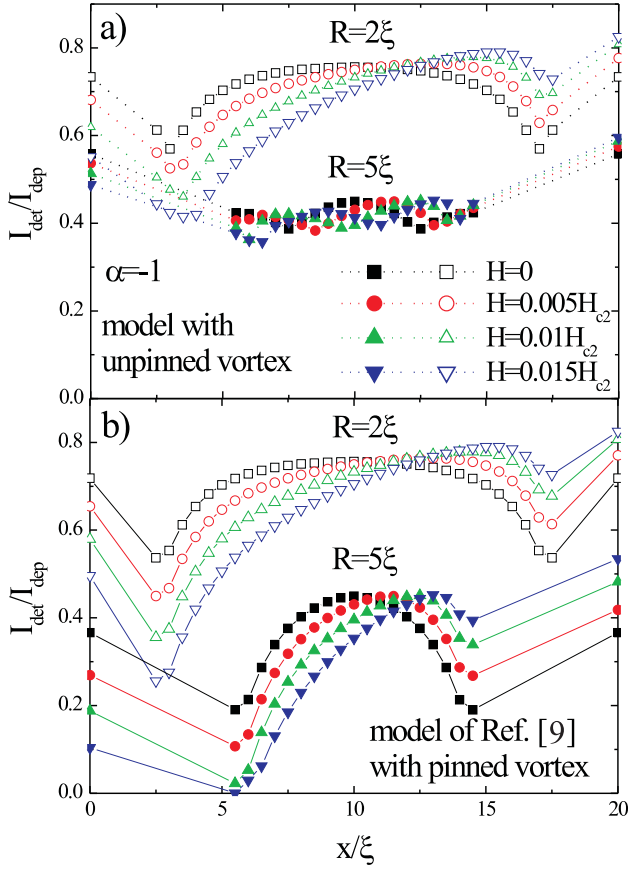


FIG. 6: Dependence of the detection current I_{det} on the coordinate of hot spot with two radii at different magnetic fields. Figure a) corresponds to the model with unpinning vortex and b) - to the model with pinned vortex of Ref. [9].

ter which is important from point of view of vortex unpinning when the hot spot is located near the same edge. When the pinning ability by HS is weak (as for the hot spot with radius $R = 2\xi$) the change of I_{det}^{min} is large and it practically follows the change of the current density at the edge of the nanowire due to external magnetic field.

The intrinsic detection efficiency at given current I in our model is determined as a photon-sensitive part of the nanowire where $I > I_{det}(x)$ [9]. In Fig. 7 we present calculated IDE at different magnetic fields (magnetic field $0.005H_{c2}$ for NbN1 detector with $\xi(T = 1.7K) = 4.9nm$ corresponds to $\simeq 69mT$) and different radii of hot spot.

First of all from Fig. 7 one can see that in both models and for all radii of the hot spot there is 'crossover' current above which IDE *decreases* while at $I < I_{cross}$ IDE *increases* with increase of the magnetic field. The first effect comes from the increase of maximal detection current I_{det}^{max} while the second effect originates from decrease of I_{det}^{min} (see Fig. 6). Secondly, in the model with pinned vortex there is strong dependence of IDE on the magnetic field (see insets in Fig. 7) for all studied radii of HS while in the model with unpinning vortex the field dependence is determined by its radius - the larger the

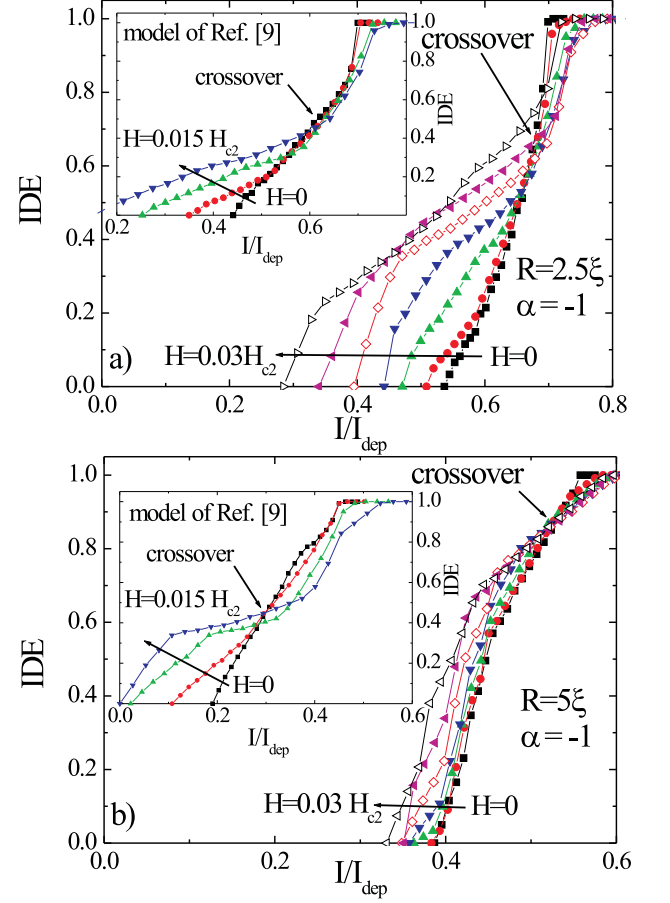


FIG. 7: Current dependence of IDE at different magnetic fields (from $H = 0$ up to $H = 0.03H_{c2}$ with step $\delta H = 0.005H_{c2}$) following from the vortex hot spot model with unpinning vortex. Figure (a) corresponds to the hot spot with radius $R = 2.5\xi$ while figure (b) to the hot spot with $R = 5\xi$ (in both cases $\alpha = -1$). In the insets similar dependencies are calculated in the hot spot model with pinned vortex of Ref. [9].

radius the weaker field dependence.

In addition we considered hot spots with *fixed* radius $R = 5\xi$ and varying coefficient α in range $0 - 0.64$, which corresponds to $\Delta_{in}=0 - 0.8\Delta_{eq}$ (in absence of transport current). We find that for all values of α there is 'crossover' current and with decreasing α field dependence of IDE(I) becomes weaker (again due to increased ability of the hot spot to pin the vortices).

We also studied how presence of edge defects may influence photon count rate and IDE. First of all we considered uniform suppression of the critical temperature along nanowire's edges (in the area with width $\delta x = \xi/2$) where we put $\alpha = -1$. Such a 'dead' layer influences quantitatively the shape of dependence IDE(I, H) (compare Fig. 7 and Fig. 8). We also calculate IDE(I, H) for

another type of the edge defect (point like suppression of T_c at the edge) and different values of coefficient α inside the hot spot. All these changes led to quantitative variation of $\text{IDE}(I, H)$ (not shown here) but qualitative properties (namely the presence of the 'crossover' current and dependence of $\text{IDE}(H)$ on the radius of the hot spot and/or Δ_{in}) stay the same.

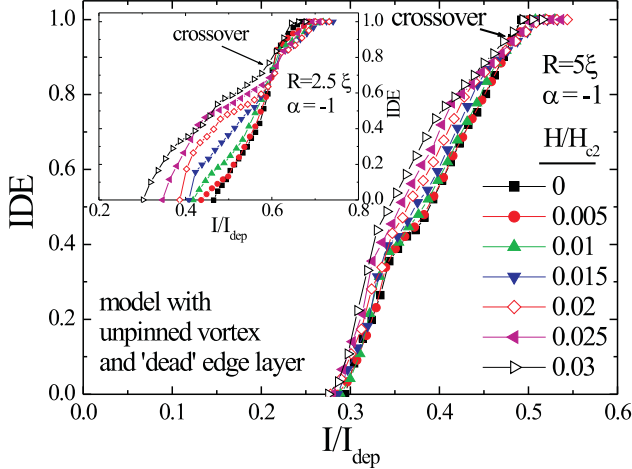


FIG. 8: Current dependence of IDE at different magnetic fields following from the vortex hot spot model with unpinned vortex and 'dead' edge layers in the nanowire, where T_c is locally suppressed.

B. Effect of meander geometry and bulk intrinsic defects

We have to stress, that the results present in Figs. 5-8 correspond to the straight nanowire, while real detectors have a form of the meander. In Fig. 9 we show calculated field dependence of the critical current of the meander with parameters close to experimental ones (see insets in Fig. 9) and straight nanowire with width $w = 20\xi$. We choose such a bend of the meander where the magnetic field suppresses the critical current (for the opposite bend or the opposite current direction the same magnetic field may enhance I_c [22]). Because of the current crowding effect $I_c(H)$ of the meander is substantially smaller than $I_c(H)$ of the straight nanowire [22] (the difference is not large at zero magnetic field but it is more pronounced at finite H) and it makes unreachable large values of IDE calculated at finite H and shown in Figs. 7-8 for straight nanowire. When current approaches $I_c(H)$ the dark counts will interfere the photon counts and SNSPD stops to work.

It is interesting to note, that according to our calculations there are no vortices in the narrowest part of the meander at $I \lesssim I_c(H)$ up to the field $H = 0.038H_{c2}$. On the contrary vortices enter the bend region at field $H \geq 0.013H_{c2}$. It occurs due to wider part of the meander in the bend region and smaller value of the critical

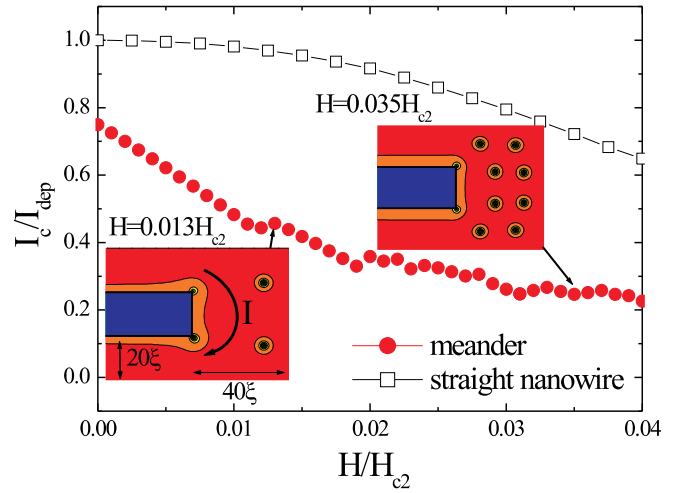


FIG. 9: Magnetic field dependence of the critical current of the straight nanowire with $w=20\xi$ (empty squares) and the meander (solid circles) with geometrical parameters shown on the bottom inset. For the meander we take into account the bend where external magnetic field decreases the critical current. In the insets we show contour plot of $|\Delta|$ for the meander at different magnetic fields and $I \lesssim I_c(H)$. At $H \leq 0.012H_{c2}$ there are no vortices in the meander. In the narrowest place of the meander vortices appear at $H > 0.038H_{c2}$.

magnetic field $H_s \simeq \Phi_0/\xi w$ at which vortices may enter superconducting nanowire [13].

As we show in the inset of Fig. 4 dependence $I_c(H)$ of real meander at $H \rightarrow 0$ may have a plateau instead of linear decay. Such a dependence is possible if somewhere in the middle of straight pieces of the meander there is relatively large intrinsic defect (where locally either T_c is suppressed or nanowire is thinner) [23]. From physical point of view the effect of intrinsic defect on I_c is similar to the effect of hot spot on I_{det} . From Fig. 6 it follows that if intrinsic defect (or hot spot) is located close to the center of straight nanowire it provides much weaker field dependence of I_c than the similar defect placed at the edge. Only when the current density (supervelocity) at the nanowire's edge exceeds (at some magnetic field) the current density (supervelocity) near the central defect then vortices start to enter the nanowire via edge (and not the vortex-antivortex pair is nucleated at the central defect) and critical current recovers strong field dependence.

Intrinsic defects may influence I_c not only at low magnetic fields but also at relatively large fields, when vortices exist in the meander at $I \lesssim I_c(H)$. Indeed, calculated $I_c(H)$ decays faster than the experimental one (compare Fig. 9 with inset in Fig. 2(d)) at the magnetic fields $H \gtrsim 0.015H_{c2}$ ($\mu_0 H \gtrsim 207\text{mT}$ for NbN1 sample) when I_c changes nonlinearly with H . Such a deviation could be explained by the vortex pinning at the intrinsic defects of the nanowire which are absent in our calculations. Similar effect was observed for NbN straight films in the recent experiment [26] and analytically it was cal-

culated in Ref. [27] for the bulk pinning described by the Bean model. Vortex pinning should prevent fast decay of I_{det}^{min} with increase of H (in this case the vortex should overcome not only the pinning by the hot spot but also the intrinsic pinning outside HS) and it has to be taken into account for quantitative comparison of experimental and theoretical IDE(I) at magnetic fields larger than $0.015H_{c2}$ ($\sim 207mT$) for detector NbN1.

Now we would like to discuss contribution of the bends to detection ability of the meander-like detectors. Because of the current crowding effect the regions near the interior corners of the bends are capable to detect photons at the currents lower than the minimal detection current I_{det}^{min} of the straight nanowire. Rough estimation, based on the difference between critical current of the meander and the straight nanowire says that near-corner area stops to detect photons at the current $I^{min} = I_{det}^{min} \cdot I_c^{meander} / I_c^{nanowire}$. This estimation works relatively well for photons which create small hot spots (with radius $R \lesssim 2\xi$) while for larger spots with small Δ_{in} it underestimates I^{min} and I^{min} lies closer to I_{det}^{min} (numerical calculations in Ref. [9] confirm it - see Fig. 12 there).

Using numerical simulations we find in what area S near the bend the local current density is larger (we use criteria $j > 1.01j_\infty$) than the current density far from the bend j_∞ . For our geometrical parameters (see Fig. 9) we find $S \simeq 400\xi^2 \sim w^2$. For parameters of NbN1 meander it consists about 1.4% of all area of the detector and it gives us the rough estimation for the photon-sensitive area at the currents just below I_{det}^{min} . When current decreases further this area shrinks as $I \rightarrow I^{min}$. Therefore we suggest that finite $0 < IDE \lesssim 0.014$ in the current range $I^{min} < I < I_{det}^{min}$ comes from this photon-sensitive area located near the interior corners of the meander. This suggestion is also supported by very weak field dependence of $IDE(H) \ll 1$ observed in our experiment at $\mu_0 H < 70mT$. If finite and small IDE would be connected with thermoactivated vortex entry (as it was assumed in [6, 9]) it should have strong field dependence in the same range of magnetic fields as a dark count rate has (see Figs. 3,4). But if our idea is correct, then IDE should not change (or change very slightly) because of presence of the *right* and *left* bends in the meander. Indeed, external magnetic field increases the current density in one kind of bend (let it be right one for definiteness) and decreases it in another one. We calculate the change in the area near both bends where current density is locally enhanced and find that this area practically does not vary at low magnetic fields because its expansion near the right bend is compensated by its shrinkage near the left bend.

C. Threshold current versus photon's energy

In Fig. 10 we show experimental dependence of the current (we call it as threshold current I_{thr}), at which IDE reaches 0.9, on the energy of the photon E . Our

choice of the cut-off is not accident. Indeed, in the bend region there is large area, where the current density is smaller than j_∞ and this part participates in photon detection at larger currents than the straight pieces of the meander. Roughly, for our geometrical parameters this area is about 10% of area of the meander. Hence, when the current approaches I_{det}^{max} of the straight nanowire the intrinsic detection efficiency of the meander reaches 0.9 and to reach IDE= 1 one should increase current further.

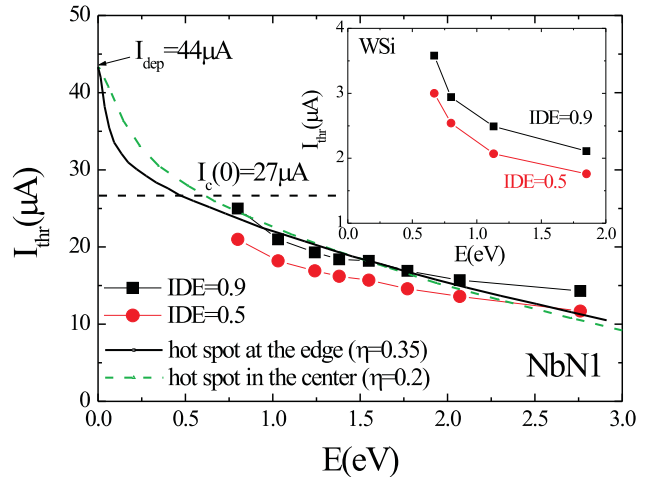


FIG. 10: Dependence of the current, at which IDE reaches 0.9 (squares) and 0.5 (circles), on the energy of the photon (results are obtained for NbN1 detector). The theoretical curves (solid and dashed) are found in assumption that current I_{thr} corresponds to the hot spot located in the center of the nanowire or at its edge (in the last case it has form of semicircle). Fitting coefficient η describes what part of the photon's energy goes for suppression of Δ inside the hot spot [28]. In the inset we show results for WSi based detector extracted from Fig. 2 of Ref. [29].

In Fig. 10 we also plot theoretical dependencies, following from the vortex hot spot model developed here. We use two locations of the hot spot (in the center and at the edge of the nanowire) and fitting parameter η , which describes what part of the energy of the photon goes for suppression of Δ inside the hot spot [28]. The quantitative agreement between the theory and the experiment is poor, which justifies that the used model assumptions are too rough. Indeed, the shape of the hot spot is not obligatory should have a round shape, because in the presence of the transport current it will preferably grow in the direction perpendicular to the current flow (due to current crowding at the equator of HS). Besides the coefficient η may depend on the energy of the photon. Both these factors are not taken in our model, because they need calculation of the dynamics of nonequilibrium quasiparticles and solution of the kinetic equation. However our model predicts nonlinear dependence of $I_{thr}(E)$ with rapid growth of I_{thr} up to I_{dep} as $E \rightarrow 0$ which resembles experimental results.

Our experimental dependence $I_{thr}(E)$ drastically differs from the linear relation found in Ref. [30] for superconducting NbN bridge. Note that very similar nonlinear dependence follows from the measurements on WSi based detector (see inset in Fig. 10 - the data were extracted from Fig. 2 of Ref. [29]). We checked that for other cut-offs (we take IDE= 0.5 and IDE= 0.01) the dependence $I_{thr}(E)$ is still nonlinear (in Fig. 10 we show results for cut-off IDE= 0.5). The reason for the difference with Ref. [30] is not clear to us.

IV. DISCUSSION

Our experimental results correlate with preceding experiments where the effect of magnetic field on photon and dark count rate in SNSPD was studied. In Refs. [31, 32] no effect of low magnetic field on PCR was observed (for TaN and NbN based detectors, respectively) while in the same range of magnetic fields the dark count rate demonstrated strong field dependence. Absence of change of PCR in Ref. [31] is probably connected with low value of the maximal magnetic field used in the experiment ($\mu_0 H_{max} = 10mT$). In Ref. [32] authors observed increase of PCR at larger magnetic fields and found that the value of the effect depends on the wavelength - the smaller λ the smaller change of PCR (the similar result was found in Ref. [14] for MoSi detector). The small *decrease* of PCR was observed in Ref. [32] (see the bump at low magnetic fields and $I = 0.78I_{c,e}$ in Fig. 3 of Ref. [32]) but this effect was not discussed in that paper.

In recent work [33] photon count rate in superconducting NbN bridge (with width $w = 150nm$) was measured at different magnetic fields and authors found field dependence of PCR at $\mu_0 H \gtrsim 30$ mT. From present in Fig. 4 of Ref. [33] experimental dependence $I_c(H)$ we may conclude that somewhere in the middle of the bridge the intrinsic defect exists and it leads to weak change of I_c at $\mu_0 H \lesssim 30mT$ (like in our NbN2 detector - see inset in our Fig. 4, but at different fields due to difference in the defects and widths). This 'weak' place most probably provides finite count rate at low currents (when IDE $\ll 1$) and PCR rapidly grows with the current increase due to expansion of the photon-sensitive area near that place (like near a bend in the meander). At $\mu_0 H \gtrsim 30$ mT experimental I_c starts to decay with increase of magnetic field which means that at these fields the weakest place is located at the edge of the bridge (due to large edge screening currents produced by applied magnetic field). It is accompanied by field dependence of the photon count rate, qualitatively similar to our experimental findings for large wavelengths. Unfortunately in Ref. [33] only one wavelength ($\lambda = 826$ nm) was used and we cannot be sure in our treatment of their results. Because in Ref. [33] PCR did not saturate at large currents the 'crossover' current could not be observed.

In Refs. [14, 32] authors compared experimental PCR(H) with prediction of the hot belt model [6] and

find large quantitative disagreement. We believe that the hot belt model of Ref. [6] is not able to explain decrease of PCR (when $PCR \simeq PCR_{sat}$ and IDE $\simeq 1$) at weak magnetic fields and stronger field dependence of PCR for photons of smaller energies (see our arguments in Introduction). These properties appear as inevitable consequences of our vortex hot spot model and they are robust with respect to the presence of edge or bulk defects which affect them only quantitatively (they may change the position of the 'crossover' current and influence quantitatively the dependence PCR(H) at relatively large magnetic fields).

Due to very weak field dependence of the photon count rate at low magnetic fields $\mu_0 H \lesssim 70mT$ for all studied wavelengths ($\lambda = 450 - 1550nm$) we conclude that fluctuation-activated vortex entry to the hot spot plays no role in the photon counting for our NbN detectors. On the contrary, the dark counts are most probably connected with fluctuation assisted vortex nucleation in the nanowire near the 'weakest' place. It is justified from the shift of current dependence of the dark count rate in magnetic field which follows the change in the critical current of the superconducting meander.

In our theoretical consideration we assume that all parts of the meander are identical. In reality there could be variations of the material (mean path length, critical temperature) or geometrical (width, thickness) parameters, which of course additionally smears dependence PCR(I) and IDE(I). But if these inhomogeneities are small we expect they will have only quantitative influence on the discussed here effects.

V. CONCLUSION

Experiment on the magnetic field dependence of photon count rate in NbN based SNSPD revealed the following three main features:

(1) At low magnetic fields ($\mu_0 H \lesssim 70mT$) PCR very weakly depends on magnetic field (for studied wavelengths $\lambda = 450 - 1550$ nm), while dark count rate has pronounced field dependence.

(2) At larger fields PCR changes with magnetic field and the smaller the energy of the photon the stronger field dependence of PCR.

(3) For all studied wavelengths there is a 'crossover' current above which PCR slightly *decreases* while at $I < I_{cross}$ PCR *increases* with increasing magnetic field. 'Crossover' current is located close to the current at which PCR(I) saturates and reaches plateau.

All observed features could be explained by the vortex hot spot model:

i) In the vortex hot spot model it is assumed that the absorbed photon creates the finite region with partially suppressed Δ (hot spot). Appearance of such a region changes the critical current of the nanowire. The resistive state starts at some detection current I_{det} via nucleation of the vortex-antivortex pair inside the HS and

their motion across the nanowire if HS is located close to the center of the nanowire. If the hot spot is located close to the edge of the nanowire the resistive state is realized via single vortex entrance via edge and its motion across the hot spot and nanowire.

ii) Detection current depends nonmonotonically on the position of the hot spot across the nanowire and has maximal I_{det}^{max} and minimal I_{det}^{min} values. Photon count rate reaches maximum when applied current becomes larger than I_{det}^{max} and PCR gradually decreases with decreasing current due to shrinkage of the photon-sensitive area.

iii) Perpendicular magnetic field induces the screening currents in the nanowire and it changes $I_{det}(x)$. Detection current decreases near the edge of the nanowire where the current density increases and I_{det} increases near the opposite edge. It leads to the shift of I_{det}^{min} to smaller currents and I_{det}^{max} to larger currents, which explains the existence of the 'crossover' current in the experiment.

iv) When the hot spot is large (in units of coherence length) and Δ is strongly suppressed inside HS it can strongly pin vortices and both I_{det}^{min} and I_{det}^{max} slightly varies at relatively low magnetic fields $H \lesssim H_s$. The hot spots with small size and/or slightly suppressed Δ produces weak pinning and detection current changes in the same magnetic fields much stronger. It explains property (2) found in the experiment.

v) In the detectors made in the form of meander there are right and left bends. At small currents and weak magnetic fields these regions are responsible for the fi-

nite photon count rate due to locally enhanced current density. With increasing magnetic field the whole area where the current density is locally enhanced both in right and left bends practically does not change because in one kind of bends current density decreases while in another it increases. The increase of photon count rate starts only when $I_{det}^{min}(H)$ of the straight part of meander approaches to the transport current.

Acknowledgments

The work was partially supported by the Russian Foundation for Basic Research (project 15-42-02365/15) and by the Ministry of education and science of the Russian Federation (the agreement of August 27, 2013, N 02.49.21.0003 between The Ministry of education and science of the Russian Federation and Lobachevsky State University of Nizhni Novgorod). The following authors acknowledge support from the Ministry of Education and Science of the Russian Federation: Yu.K. (unique identifier of the scientific research RFMEFI58614x0007), A.K. (State contract No.14.B25.31.0007), A.S. (state task No. 2327) and G.G. (state task No. 960). A.S. also acknowledges support by grant of the President of the Russian Federation (contract No. MK-6184.2014.2), and G.G. acknowledges support by grant of the President of the Russian Federation (contract No. NSH-1918.2014.2).

-
- [1] A. D. Semenov, G. N. Gol'tsman, and A. A. Korneev, Phys. C (Amsterdam) **351**, 349 (2001).
 - [2] G. Gol'tsman, O. Okunev, G. Chulkova, A. Lipatov, A. Semenov, K. Smirnov, B. Voronov, A. Dzardanov, C. Williams, and R. Sobolewski, Appl. Phys. Lett. **79**, 705–707 (2001).
 - [3] A. Semenov, A. Engel, H.-W. Hübers, K. Il'in, and M. Siegel, Eur. Phys. J. B **47**, 495 (2005).
 - [4] L. Maingault, M. Tarkhov, I. Florya, A. Semenov, R. Espiau de Lamaestre, P. Cavalier, G. Gol'tsman, J.-P. Poizat, and J.-C. Villégier, J. Appl. Phys. **107**, 116103 (2010).
 - [5] A. Zotova and D. Y. Vodolazov, Phys. Rev. B **85**, 024509 (2012).
 - [6] L. N. Bulaevskii, M. J. Graf, and V. G. Kogan, Phys. Rev. B **85**, 014505 (2012).
 - [7] A. Eftekharian, H. Atikian, and A. H. Majedi, Opt. Express **21**, 3043 (2013).
 - [8] A. Engel and A. Schilling, J. Appl. Phys. **114**, 214501 (2013).
 - [9] A. Zotova and D. Y. Vodolazov, Supercond. Sci. Technol. **27**, 125001 (2014).
 - [10] C. M. Natarajan, M. G. Tanner, and R. H. Hadfield, Supercond. Sci. Technol. **25**, 063001 (2012).
 - [11] A. Rothwarf and B. N. Taylor, Phys. Rev. Lett. **19**, 27 (1967).
 - [12] M. Tinkham, *Introduction to superconductivity*, (McGraw-Hill, NY, 1996).
 - [13] G. Stejic, A. Gurevich, E. Kadyrov, D. Christen, R. Joynt, and D.C. Larbalestier, Phys. Rev. B **49**, 1274 (1994).
 - [14] A. A. Korneev, Y. P. Korneeva, M. Y. Mikhailov, Y. P. Pershin, A. V. Semenov, D. Y. Vodolazov, A. V. Divochiy, Y. B. Vakhtomin, K. V. Smirnov, A. G. Sivakov, A. Y. Devizenko, and G. N. Goltsman, IEEE Transactions on Applied Superconductivity, **25**, 6975120 (2015).
 - [15] C. Qiu and T. Qian, Phys. Rev. B **77**, 174517 (2008).
 - [16] H. Bartolf, A. Engel, A. Schilling, H.-W. Hubers and A. Semenov, Phys. Rev. B **81**, 024502 (2010).
 - [17] L. N. Bulaevskii, M. J. Graf, C. D. Batista and V. G. Kogan, Phys. Rev. B **83**, 144526 (2011).
 - [18] D. Y. Vodolazov, Phys. Rev. B **85**, 174507 (2012).
 - [19] B. I. Ivlev, S. G. Lisitsyn, and G. M. Eliashberg, J. Low Temp. Phys. **10**, 449 (1973).
 - [20] A. I. Larkin and Yu. N. Ovchinnikov, Sov. Phys. JETP **41**, 960 (1976).
 - [21] L. Kramer and R.J. Watts-Tobin, Phys. Rev. Lett. **40**, 1041 (1978).
 - [22] J. R. Clem, Y. Mawatari, G.R. Berdiyrov and F.M. Peeters, Phys. Rev. B **85**, 144511 (2012).
 - [23] One should have in mind that plateau like dependence of $I_c(H)$ at $H \rightarrow 0$ may exist if there is no intrinsic defect in central part of the nanowire (see Fig. 9 for straight nanowire). It appears when $I_c(0) \simeq I_{dep}$ [24, 25] due to

- depairing effect of superconducting current (supervelocity). But in our detectors $I_c(0)$ is far below I_{dep} (see table 1) and this effect could be skipped.
- [24] G. M. Maksimova, N. V. Zhelezina and I. L. Maksimov, Europhys. Lett. **53**, 639 (2001).
 - [25] V.P. Andratskii, L.M. Grundel', V.N. Gubankov, and N.B. Pavlov, Zh. Eksp. Teor. Fiz. **65**, 1591 (1973) [Sov. Phys. JETP **38**, 797 (1974)].
 - [26] K. Ilin, D. Henrich, Y. Luck, Y. Liang, M. Siegel, D. Yu. Vodolazov, Phys. Rev. B **89**, 184511 (2014).
 - [27] A.A. Elistratov, D.Y. Vodolazov, I.L. Maksimov, J.R. Clem, Phys. Rev. B **66**, 220506 (2002).
 - [28] D.Yu. Vodolazov, Phys. Rev. B **90**, 054515 (2014).
 - [29] B. Baek, A. E. Lita, V. Verma, and S. W. Nam, Appl. Phys. Lett. **98**, 251105 (2011).
 - [30] J. J. Renema, R. Gaudio, Q. Wang, Z. Zhou, A. Gaggero, F. Mattioli, R. Leoni, D. Sahin, M. J. A. de Dood, A. Fiore, and M. P. van Exter, Phys. Rev. Lett. **112**, 117604 (2014).
 - [31] A. Engel, A. Schilling, K. Il'in and M. Siegel, Phys. Rev. B **86**, 140506(R) (2012).
 - [32] R. Lusche, A. Semenov, Y. Korneeva, A. Trifonov, A. Korneev, G. Gol'tsman, and H.-W. Hübers, Phys. Rev. B **89**, 104513 (2014).
 - [33] J. J. Renema, R. J. Rengelink, I. Komen, Q. Wang, R. Gaudio, K. P. M. op't Hoog, Z. Zhou, D. Sahin, A. Fiore, P. Kes, J. Aarts, M. P. van Exter, M. J. A. de Dood, and E. F. C. Driessen, Appl. Phys. Lett. **106**, 092602 (2015).